



# Surface morphology and magnetic properties in $\text{Pr}_{0.7}\text{Sr}_{0.3}\text{MnO}_3$ layer grown on charge-ordered $\text{La}_{0.5}\text{Ca}_{0.5}\text{MnO}_3$ layer



Haiou Wang<sup>a,b,\*</sup>, Chunyu Song<sup>a</sup>, Kunpeng Su<sup>a</sup>, Dexuan Huo<sup>a,\*\*</sup>, Weishi Tan<sup>b</sup>

<sup>a</sup> Institute of Materials Physics, Hangzhou Dianzi University, Hangzhou 310018, China

<sup>b</sup> Key Laboratory of Soft Chemistry and Functional Materials, Ministry of Education, Department of Applied Physics, Nanjing University of Science and Technology, Nanjing 210094, China

## ARTICLE INFO

### Article history:

Received 23 September 2015

Received in revised form 9 December 2015

Accepted 21 December 2015

Available online 23 December 2015

### Keywords:

Magnetic materials  
Multilayer structure  
Surfaces  
Interfaces

## ABSTRACT

We report magnetic behaviors in  $\text{Pr}_{0.7}\text{Sr}_{0.3}\text{MnO}_3$  (PSMO) layer grown on charge-ordered  $\text{La}_{0.5}\text{Ca}_{0.5}\text{MnO}_3$  (LCMO) layer. PSMO/LCMO bilayer film was prepared by pulsed laser deposition on  $\text{SrTiO}_3$  (001) substrate. Large particulates at the surface of PSMO layer impart inhomogeneous composition in film, resulting in the variation of film's crystalline structure. We find an exchange bias (EB) in the bilayer film with relative roughness and inhomogeneous surface, whereas smooth and homogeneous surface does not lead to an EB effect. It is believed that an antiferromagnetic structure is formed in the inhomogeneous PSMO layer, which causes the EB effect in this system. The present results are discussed and possible explanations are provided based on the random-field model of EB and the related research results.

© 2015 Elsevier B.V. All rights reserved.

## 1. Introduction

A large variety of extraordinary properties have been discovered in oxide materials, such as colossal magnetoresistance (CMR) [1–3] in perovskite manganese oxides of composition  $R_{1-x}A_x\text{MnO}_3$  ( $R$  = rare earth,  $A$  = alkaline earth) or high- $T_C$  superconductivity [4]. CMR is often observed in a large range of doping  $x$ . For  $0.2 < x < 0.45$ , many compounds exhibit a ferromagnetic (FM) metallic phase below their Curie temperature  $T_C$  while presenting a semiconductor-like behavior in their paramagnetic phase at high temperature. The application of a magnetic field generates a magnetoresistance (MR) near this metal-insulator transition. Half-doped manganite  $\text{La}_{0.5}\text{Ca}_{0.5}\text{MnO}_3$  (LCMO) [5] exhibits phase separated state and CO insulating state, which can turn into a metallic and FM phase via exerting magnetic field and introducing stress [6,7]. Due to recent improvement in thin-film deposition technique such as pulsed laser deposition (PLD), combining two materials with different properties in a system can lead to many interesting and novel effects [8–10]. The interfaces are complex especially when two competing ground states (the FM metallic state and the CO insulating state) are present [11]. Therefore, a FM  $\text{Pr}_{0.7}\text{Sr}_{0.3}\text{MnO}_3$  (PSMO) layer grown on a CO LCMO layer to form FM/CO heterostructure should be appropriate for investigation.

The advanced thin film device often crucially depends on the microstructure such as surface morphology, interlayer roughness and growth

orientation. Surface and interface affect significantly the physical properties of manganite film. In this work, we study microstructure and magnetic properties of PSMO/LCMO. Our magnetic and structural measurements suggest a correlation between surface and interfacial structure and magnetic properties. We find an exchange bias (EB) effect, i.e., a shift of the hysteresis curves, in the bilayer film with relative inhomogeneous surface. Our study suggests that large particulates at surface can impart AFM structure to the FM PSMO layer and then induce the AFM/FM coupling leading, in turn, to the EB in this system.

## 2. Experimental details

Epitaxial PSMO (36 nm)/LCMO (24 nm) bilayer structure with PSMO as top layer was fabricated on single crystalline  $\text{SrTiO}_3$  (STO) (001) substrate by pulsed laser deposition (PLD, Twente Solid State Technology BV) [12]. For the PLD growth, an excimer laser with  $4.4 \times 10^{-4}$  248 nm, a repetition rate of 2 Hz, and an energy density of  $3 \text{ J/cm}^2$  were used. The base pressure in the growth chamber was pumped to  $2 \times 10^{-5}$  mbar. During the deposition, the deposition temperature is  $720^\circ\text{C}$ , the oxygen pressure is  $5 \times 10^{-1}$  mbar, and the deposition rate is  $\sim 2.4 \text{ \AA/s}$  for both materials. After deposition, the film was annealed in 1 atm pure oxygen for half an hour and cooled down slowly in the same oxygen pressure to avoid possible oxygen deficiency. Wavelength dispersive X-ray spectroscopy (LambdaSpec, EDAX Inc.) suggests that the composition of the PSMO and/or LCMO layer is the same as that of corresponding target within experimental error. Surface morphology was measured by atomic force microscopy (CSPM5500, Benyuan Nano Inc.) and the crystal structures were examined by high resolution X-ray diffraction (HRXRD). HRXRD diffraction experiments were

\* Corresponding author at: Institute of Materials Physics, Hangzhou Dianzi University, Hangzhou 310018, China.

\*\* Corresponding author.

E-mail addresses: [wanghaiou@hdu.edu.cn](mailto:wanghaiou@hdu.edu.cn) (H. Wang), [dxhuo@hdu.edu.cn](mailto:dxhuo@hdu.edu.cn) (D. Huo).

performed at Beijing Synchrotron Radiation Facility (BSRF). The X-ray wavelength is 0.15405 nm and the energy resolution is  $4.4 \times 10^{-4}$ . Magnetic characterization was carried out in Physical Property Measurement System (PPMS-9T, Quantum Design Inc.) with a vibrating sample magnetometer (VSM) option.

### 3. Results and discussion

Fig. 1 shows room-temperature HRXRD in the  $\theta$ - $2\theta$  mode of PSMO/LCMO bilayer film. Besides the reflection from STO substrate, (002) diffraction peaks of PSMO layer and LCMO layer are visible, suggesting the epitaxial relationship between the two layers in relation to the substrate. The out-of-plane lattice parameter ( $a$ ) and the corresponding strain ( $\varepsilon$ ) of PSMO layer and LCMO layer can be calculated from the HRXRD curve (see Fig. 1). The out-of-plane strain  $\varepsilon$  can be calculated using the formula  $\varepsilon = (a - a_0)/a_0$ , where  $a_0$  is the bulk unstressed lattice parameter as measured from power XRD pattern [12]. For PSMO, the out-of-plane strain value ( $\varepsilon = -1.26\%$ ) shows slight out-of-plane compression of the PSMO lattice, indicating that PSMO layer has an in-plane tensile strain. In the same way, for LCMO, the out-of-plane strain value ( $\varepsilon = -2.51\%$ ) suggests that LCMO layer has an in-plane tensile strain. Therefore, the bilayer film has an in-plane tensile strain. Interestingly, there exists a shoulder peak S1 (see Fig. 1). In inset of Fig. 1, we can see a smooth surface with root mean square (rms) roughness  $\sim 2.62$  nm. The presence of large particulates (near top right-hand corner) in atomic force microscopy image represents an atomic collapse model [13]. The total volume fraction of the particulates is about 6.25%. Such surface large particulates are typically observed in PLD-deposited films and are usually related with non-stoichiometric deposition in island-growth film [14,15]. These large particulates at surface can impart inhomogeneous composition to the film, inducing the variation of crystalline structure (see peak S1).

Fig. 2 shows the zero field-cooling (ZFC) and field-cooling (FC) temperature-dependent magnetization measurements. A characteristic temperature  $T^* \sim 54$  K is indicated with arrow in Fig. 2. Undesirable magnetization starts to decrease with further decrease of temperature at temperature  $T^*$ . This may be associated with the inhomogeneous magnetic phase induced by inhomogeneous composition in the bilayer film. Inhomogeneous composition has been shown to induce chemical or magnetic phase transition easily [16], which proves important role of inhomogeneities in determining magnetic properties. Moreover, anomaly magnetization with sharp decrease at 10 K under cooling field occurred. The large drop of magnetization in FC case probably

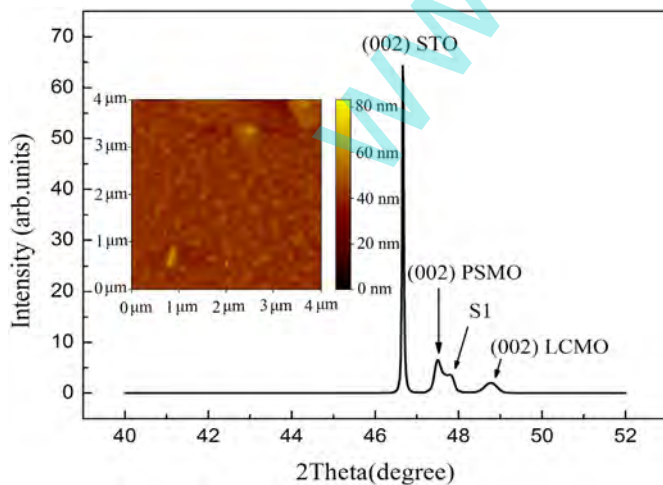


Fig. 1. HRXRD  $\theta$ - $2\theta$  scan centered on the STO (002) peak for PSMO/LCMO bilayer film on (001) STO substrate. Inset: atomic force microscopy contact mode image plotted for an area of  $4 \times 4 \mu\text{m}^2$  of PSMO/LCMO film.

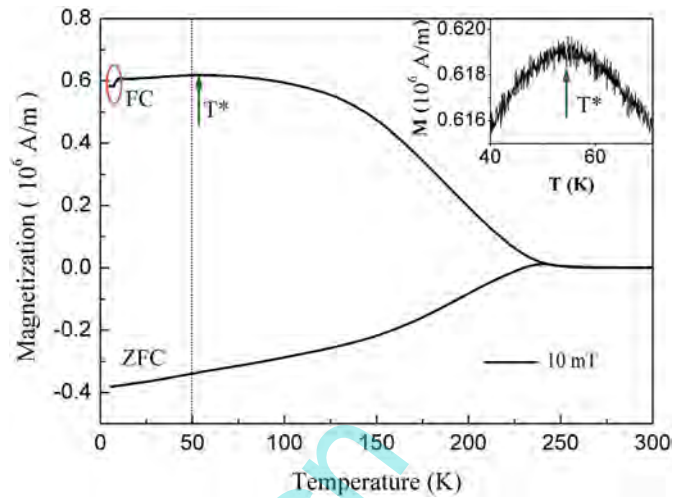


Fig. 2. Temperature dependence of magnetization with ZFC and FC in 10 mT field processes for PSMO/LCMO film. Inset was the enlarged magnetization curves.

correlates with thermal instability of a statistical distribution of magnetic domains in film.

Fig. 3 shows FC magnetic hysteresis loops, measured after cooling the film in 50 mT from 300 K down to 3 K, 50 K, 100 K and 200 K. Saturation magnetization ( $M_s$ ) monotonously increases with decreasing temperature from 200 K. However, it starts to decrease slowly with further decreasing temperature at lower than 50 K. This temperature is coincident with  $T^*$  which is corresponding to the magnetization change in Fig. 2, confirming the important role of surface particulates in decreasing ferromagnetism.

Further, we measured the ZFC and FC hysteresis loops, measured after cooling the film without and with a 50 mT field from 300 K down to 3 K and 200 K. In Fig. 4(a), a small shift of the center of the hysteresis curve along the field axis at 3 K is observed after FC in 50 mT field. While for the ZFC process, the hysteresis is normal. The exchange bias field ( $H_{EB}$ ) and coercive field ( $H_C$ ) are defined as  $H_{EB} = (|H_1| - |H_2|)/2$  and  $H_C = (|H_1| + |H_2|)/2$ , where  $H_1$  and  $H_2$  is the left and right coercive field, respectively. The  $H_{EB}$  of 7.8 mT and  $H_C$  of 28.6 mT are obtained at 3 K, whereas, the EB effect disappears at 200 K, as shown in Fig. 4(b). According to the random-field model of EB proposed by Malozemoff [17],  $H_{EB} \propto \frac{f_j J}{2M_f d_{FM}^2}$ , where  $M_f$  and  $d_{FM}$  is the magnetization

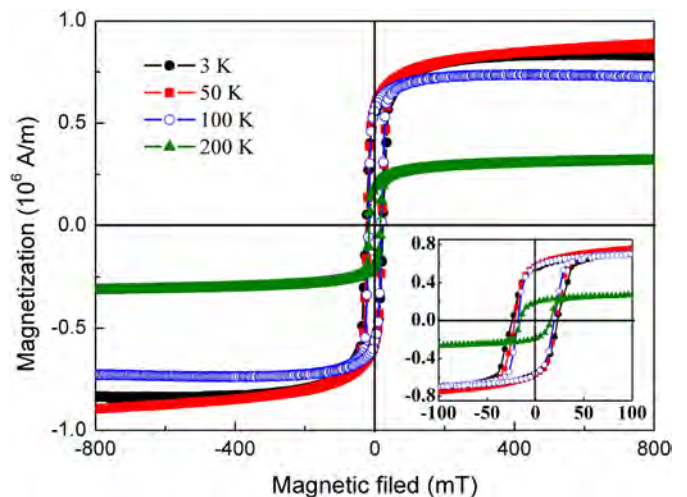


Fig. 3. The FC hysteresis loops of the PSMO/LCMO film at 3 K, 50 K, 100 K and 200 K. Inset shows low field magnetization behavior.

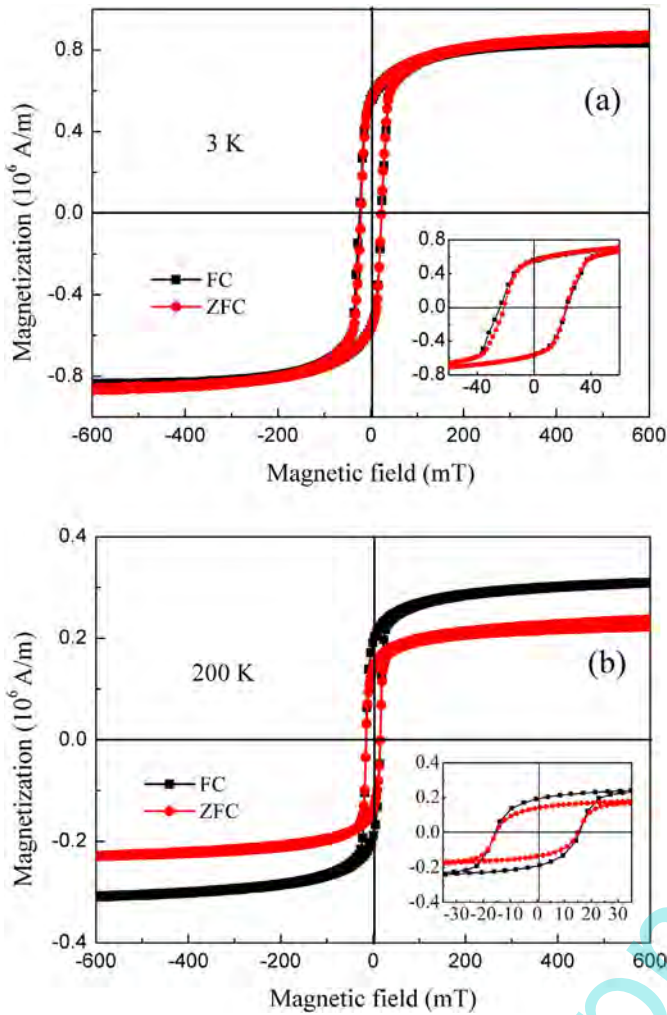


Fig. 4. Magnetic hysteresis loops of PSMO/LCMO film at 3 K (a) and 200 K (b) measured after ZFC and FC in 50 mT field. Insets show low field magnetization behavior.

and thickness of the ferromagnet, respectively,  $f_i$  is a parameter associated with randomness of spin orientations with order unity,  $J$  is the atomic exchange coupling at interface,  $a$  is the atomic spacing, and  $L$  is

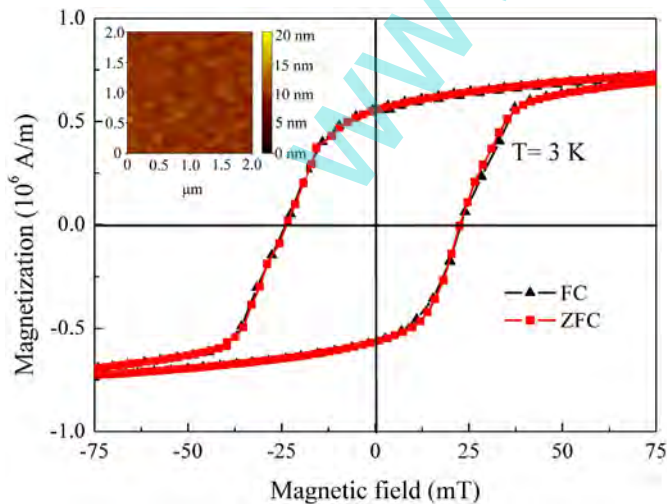


Fig. 5. Magnetic hysteresis loops of the homogeneous bilayer at 3 K measured after ZFC and FC in 50 mT field. Insets show atomic force microscopy contact mode image plotted for an area of  $2 \times 2 \mu\text{m}^2$  of the bilayer.

the domain size. Enhanced ferromagnetism ( $M_f$ ) resulting from phase separation and FM cluster percolation at PSMO/LCMO interface probably leads to the disappearance of EB at 200 K (see Fig. 4(b)). Interestingly, EB can be observed at 3 K (see Fig. 4(a)). On one hand, the large particulates at the surface of PSMO layer can produce inhomogeneous composition. Such large particulates are disordered compared to the core FM PSMO layer. The disordered shell particulates can also act as AFM on the core FM layer. The coexistence of the FM structure and AFM structure will lead to the natural FM/AFM interface. Hence, the magnetic coupling between AFM phase and FM phase gives rise to EB effect. On the other hand, the surface large particulates can impart inhomogeneous magnetic phase, leading to the decrease in  $M_f$  at  $T < T^*$  (see Fig. 2) and therefore enhancing the  $H_{EB}$ . Moreover, we have obtained a homogeneous PSMO/LCMO bilayer without surface particulates for comparison by controlling the growth condition of the film, i.e. lower the film's deposition rate and tune the cooling rate of substrate temperature. The growth was followed by an in situ fast cooling ( $35 \text{ }^\circ\text{C}/\text{min}$ ) from 720 to 500  $^\circ\text{C}$ , followed by a  $5 \text{ }^\circ\text{C}/\text{min}$  cooling ramp from 500 to 300  $^\circ\text{C}$ , and the deposition rate was changed to 0.6  $\text{\AA}/\text{s}$  for both materials. Magnetic measurements show that the EB effect cannot be observed at a low temperature  $\sim 3$  K in this homogeneous PSMO/LCMO bilayer, as shown in Fig. 5. During the preparation of film, sufficient oxygen pressure has been used to prevent the occurrence of oxygen deficiency. Here the influence of oxygen deficiency on the EB is minimal, and negligible. Thus, the EB effect should be ascribed to the surface inhomogeneity. In our previous report [18], the EB effect cannot be observed. The disappearance of EB correlates with the enhancement of  $M_f$  due to metallic FM cluster percolation at PSMO/LCMO interface. Unlike previous research, surface is abnormal and relative inhomogeneous in our PSMO/LCMO bilayer film (see inset of Fig. 1). This will reduce  $M_f$  and therefore increase  $H_{EB}$ . It is believed that an AFM structure is formed at the surface of PSMO/LCMO film, which causes the EB effect in this system.

#### 4. Conclusions

We have prepared PSMO/LCMO bilayer film by PLD. The variation of crystalline structure occurred due to surface large particulates in the film. AFM structures are formed in the inhomogeneous bilayer film, causing the EB effect at 3 K. We present a possible scenario as an explanation for the EB by a combination of surface morphology and FM cluster percolation at PSMO/LCMO interface. Our observation opens up possibilities in developing thin film oxides with tuned magnetic properties, particularly EB.

#### Acknowledgments

We acknowledge the help from colleagues at the Shanghai Synchrotron Radiation Facility and Beijing Synchrotron Radiation Facility. This work was supported by the National Natural Science Foundation of China (Grant Nos. 11574066, 51372058, U1332106) and the Scientific Research Foundation of Hangzhou Dianzi University (No. KYS205614013).

#### References

- [1] Y. Tokura, Critical features of colossal magnetoresistive manganites, *Rep. Prog. Phys.* 69 (2006) 797.
- [2] M. Španková, A. Rosová, E. Dobročka, Š. Chromík, I. Vávra, V. Štrbík, D. Machajdik, A.P. Kobzev, M. Sojková, Structural properties of epitaxial  $\text{La}_{0.67}\text{Sr}_{0.33}\text{MnO}_3$  films with increased temperature of metal–insulator transition grown on  $\text{MgO}$  substrate, *Thin Solid Films* 583 (2015) 19.
- [3] Q.Y. Xie, X.S. Wu, J. Li, B. Lv, J. Gao, Probing the dead layer thickness and its effect on the structure and magnetic properties in  $\text{La}_{2/3}\text{Ca}_{1/3}\text{MnO}_3$  thin films, *Thin Solid Films* 545 (2013) 89.
- [4] C. Chappert, A. Fert, F. Nguyen Van Dau, The emergence of spin electronics in data storage, *Nat. Mater.* 6 (2007) 813.

- [5] P. Amirzadeh, H. Ahmadvand, P. Kameli, B. Aslibeiki, H. Salamati, A.G. Gamzatov, A.M. Aliev, I.K. Kamilov, Phase separation and direct magnetocaloric effect in  $\text{La}_{0.5}\text{Ca}_{0.5}\text{MnO}_3$  manganite, *J. Appl. Phys.* 113 (2013) 123904.
- [6] Y. Takamura, F. Yang, N. Kemik, E. Arenholz, M.D. Biegalski, H.M. Christen, Competing interactions in ferromagnetic/antiferromagnetic perovskite superlattices, *Phys. Rev. B* 80 (2009), 180417(R).
- [7] S.J. May, P.J. Ryan, J.L. Robertson, J.-W. Kim, T.S. Santos, E. Karapetrova, J.L. Zarestky, X. Zhai, S.G.E. te Velthuis, J.N. Eckstein, S.D. Bader, A. Bhattacharya, Enhanced ordering temperatures in antiferromagnetic manganite superlattices, *Nat. Mater.* 8 (2009) 892.
- [8] J.F. Ding, O.I. Lebedev, S. Turner, Y.F. Tian, W.J. Hu, J.W. Seo, C. Panagopoulos, W. Prellier, G. Van Tendeloo, T. Wu, Interfacial spin glass state and exchange bias in  $\text{La}_{0.7}\text{Sr}_{0.3}\text{MnO}_3/\text{SrMnO}_3$  bilayers, *Phys. Rev. B* 87 (2013) 054428.
- [9] M. Jungbauer, S. Huehn, M. Michelmann, E. Goering, V. Moshnyaga, Exchange bias in  $\text{La}_{0.7}\text{Sr}_{0.3}\text{MnO}_3/\text{SrMnO}_3/\text{La}_{0.7}\text{Sr}_{0.3}\text{MnO}_3$  trilayer, *J. Appl. Phys.* 113 (2013), 17D709.
- [10] P. Zubko, S. Gariglio, M. Gabay, P. Ghosez, J.M. Triscone, Interface physics in complex oxide heterostructures, *Annu. Rev. Condens. Matter. Phys.* 2 (2013) 141.
- [11] A. Moreo, S. Yunoki, E. Dagotto, Phase separation scenario for manganese oxides and related materials, *Science* 283 (1999) 2034.
- [12] H.O. Wang, K.P. Su, Y.Q. Cao, L.W. Li, D.X. Huo, W.S. Tan, F. Xu, Q.J. Jia, J. Gao, Effect of surface inhomogeneities on crystalline structure and magnetic properties of epitaxial  $\text{Pr}_{0.7}\text{Sr}_{0.3}\text{MnO}_3/\text{La}_{0.5}\text{Ca}_{0.5}\text{MnO}_3$  film on (001)  $\text{SrTiO}_3$ , *Appl. Phys. A* 119 (2015) 609.
- [13] R. Cai, Y. Wang, X. Liu, W. Gao, Y. Chen, J. Sun, Y. Wang, Origin of different growth modes for epitaxial manganite films, *J. Am. Ceram. Soc.* 96 (2013) 1660.
- [14] J. Jeon, H.S. Alagoz, J. Jung, K.H. Chow, Surface inhomogeneities and the electronic phase separated states in thin films of  $\text{La}_{0.35}\text{Pr}_{0.35}\text{Ca}_{0.3}\text{MnO}_3$ , *J. Appl. Phys.* 115 (2014) 233907.
- [15] P. Abellán, C. Moreno, F. Sandiumenge, X. Obradors, M.-J. Casanove, Misfit relaxation of thin films by a nanodot segregation mechanism, *Appl. Phys. Lett.* 98 (2011) 041903.
- [16] M. Valant, T. Kolodiazny, I. Arcon, F. Aguesse, A.-K. Axelsson, N.M. Alford, Response to “Comment on the origin of magnetism in Mn-doped  $\text{SrTiO}_3$ ” *Adv. Funct. Mater.* 23 (2013) 2231.
- [17] A.P. Malozemoff, Mechanisms of exchange anisotropy, *J. Appl. Phys.* 63 (1988) 3874.
- [18] H. Wang, J. Zhang, Q. Jia, F. Xu, W. Tan, D. Huo, J. Gao, Three-dimensional strain state and spacer thickness-dependent properties of epitaxial  $\text{Pr}_{0.7}\text{Sr}_{0.3}\text{MnO}_3/\text{La}_{0.5}\text{Ca}_{0.5}\text{MnO}_3/\text{Pr}_{0.7}\text{Sr}_{0.3}\text{MnO}_3$  trilayers, *J. Appl. Phys.* 115 (2014) 233911.